34th Annual International Conference of the IEEE EMBS
San Diego, California USA, 28 August - 1 September, 2012

Motion Artifact Reduction in Electrocardiogram using Adaptive Filtering Based on Half Cell Potential Monitoring

Byung-hoon Ko, Takhyung Lee, Changmok Choi, Youn-ho Kim, Gunguk Park, KyoungHo Kang, Sang Kon Bae, Kunsoo Shin, *Member, IEEE*

***Abstract*— The electrocardiogram (ECG) is the main measurement parameter for effectively diagnosing chronic disease and guiding cardio-fitness therapy. ECGs contaminated by noise or artifacts disrupt the normal functioning of the automatic analysis algorithm. The objective of this study is to evaluate a method of measuring the HCP variation in motion artifacts through direct monitoring. The proposed wearable sensing device has two channels. One channel is used to measure the ECG through a differential amplifier. The other is for monitoring motion artifacts using the modified electrode and the same differential amplifier. Noise reduction was performed using adaptive filtering, based on a reference signal highly correlated with it. Direct measurement of HCP variations can eliminate the need for additional sensors.**

I. Introduction

The number of patients with chronic diseases is constantly increasing. Cardiovascular disease in particular, including hypertension and heart disease, is prevalent in as much as 19.6% of the population, one report showed [1]. Medical expenses are rising as the population ages and more people develop chronic cardiovascular diseases such as high blood pressure and heart disease. Patient-specific disease management and exercise are helpful in reducing the expense and improving the quality of healthcare.

Recently, connected healthcare systems using wireless biological monitoring devices, gateway servers, and data servers have been applied to various healthcare services, such as family healthcare and elderly patient care [2][3]. To monitor signs of cardiovascular disease, the convergence of mobile devices (smartphones and tablet PCs) and wearable sensors to measure physiological signals have been pursued more actively.

The electrocardiogram (ECG) is the main measurement parameter for effectively diagnosing chronic disease and guiding cardio-fitness therapy. For observing cardiac arrhythmias, a halter monitor is used for continuously monitoring ECG for more than 24 hours. An arrhythmia detection algorithm is useful in that it relieves the M.D.'s labors by delivering just the pertinent ECG information, including any signs of arrhythmia, with automatic annotation. To ensure that exercises are effective, during aerobic exercise, a heart-rate monitor provides the user with information such as the specific heart-rate zone, calories burned, and breathing rate.

ECGs contaminated by noise or artifacts disrupt the normal functioning of the automatic analysis algorithm. Noise and artifacts are caused by several factors, such as power-line interference, skin-electrode motion artifacts, and electromyography noise [4]. Artifacts in ECGs can mimic the frequency bands and morphologies of interesting features. Analyses of these artifact-impaired, low-quality signals can therefore generate false positives or false negatives.

Before attempting signal processing, it is important to acquire an ECG with a high signal-to-noise ratio by optimally positioning sensors and preparing skin surfaces for their attachment. Beyond this, however, adding adaptive filtering using a reference signal has been proposed, to estimate and remove the inevitable occurrence of motion artifacts. The reference signal measures motion artifacts by means of various sensors (a strain gauge, optical sensor, and accelerometer) [5][6][7][8]. Indirectly measured reference signals show a low correlation with motion artifacts because they yield inaccurate estimates of the electrical characteristics of the skin/electrode interface. This low correlation results from the accumulated errors in field changes, errors created by estimation and approximation.

In the author's previous study, noise caused by impedance changes in the skin–electrode interface was calculated using a lumped-parameter impedance model. The effect of motion-induced deformation of the skin–electrode interface was extremely small because the model did not include the variation of the half-cell potential in the electrical double layer [9].

Half-cell potential (HCP), a major factor in the production of motion artifacts, is described by the simplified model of the Gouy-Chapman-Stern model of the double layer. In this model, the potential can be calculated by the change rate of the metal electrode's area while it is in the electrolyte [10]. Therefore, measurements related to areal changes are needed in order to accurately predict artifacts induced by motion.

The objective of this study is to evaluate a method of measuring the HCP variation in motion artifacts through direct monitoring. Noise reduction was performed using

B. Ko is with the Future IT Research Center, Samsung Advanced Institute of Technology (SAIT), Samsung Electronics Co., Ltd., Yongin, Republic of Korea (phone: +82-31-280-6538; fax: +82-31-280-9560; e-mail: byunghoon.ko@samsung.com).

T. Lee, C. Choi, Y. Kim, G Park, K Kang, S Bae and K. Shin are with the Future IT Research Center, Samsung Advanced Institute of Technology (SAIT), Samsung Electronics Co., Ltd., Yongin, Republic of Korea (e-mail: takhyung.lee@samsung.com, cm7.choi@samsung.com, yh92.kim@samsung.com, ggpark@samsung.com, kyoungho.kang@samsung.com, sk111.bae@samsung.com and bosco.shin@samsung.com).

adaptive filtering, based on a reference signal highly correlated with it. Direct measurement of HCP variations can eliminate the need for additional sensors.

II. METHOD

The proposed wearable sensing device has two channels. One channel is used to measure the ECG through a differential amplifier. The other is for monitoring motion artifacts using the modified electrode and the same differential amplifier.

A. Electrical circuit model of skin/electrode interface

A biopotential is measured as the difference in readings between two electrodes. The equivalent circuit model for the bipolar electrode pair on a body surface is shown in Fig 1.

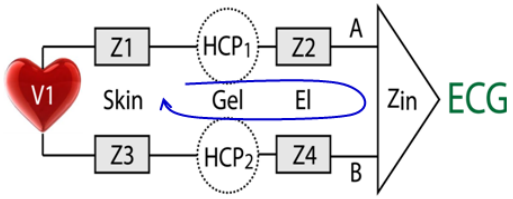

Figure 1. Electrical circuit model for ECG CH

The measurement of the first amplifier ECG is given by (1).

$$ECG = V_1^+ \times \frac{Zin}{Z_1 + Z_2 + Zin} - V_1^- \times \frac{Zin}{Z_3 + Z_4 + Zin} + HCP_1 \times \frac{Zin}{Z_1 + Z_2 + Zin} - HCP_2 \times \frac{Zin}{Z_3 + Z_4 + Zin} \quad (1)$$

Where Z_i is the impedance of each layer of the skin–electrode interface and HCP_i is the half-cell potential between the electrode and electrolyte. The half-cell potential value varies depending on the electrode material. Ideally, if $Z_1 + Z_2$ and $Z_3 + Z_4$ are the same, the half-cell potential values (HCP_1, HCP_2) are cancelled out.

B. Electrical Circuit Model of HCP electrode

The modified bipolar electrode having Z5 can block ECG readings from the heart, as shown in Fig 2.

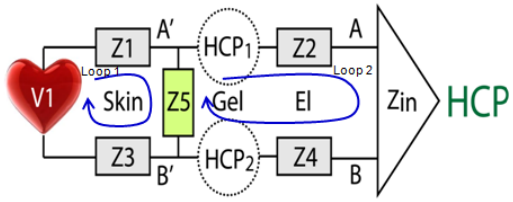

Figure 2. Electrical circuit model for HCP CH

The HCP channel can directly measure HCP changes in the same signal path as the ECG's. In the signal path from heart to amplifier, two loops are formed by Z5. Two governing equations for the differential potential in each loop can be derived as follows:

In 1st loop

$$A`-B` = (V_1^+ - V_1^-) \times \frac{Z5}{Z1 + Z3 + Z5} \cong 0 \quad if \quad Z5 \cong 0 \quad (2)$$

In 2nd loop

$$i = \frac{A`-B`+HCP_1 + HCP_2}{Z_2 + Zin + Z_4 + Z_5}$$

$$HCP = A - B = Zin \times i = Zin \times \frac{A`-B`+HCP_1 + HCP_2}{Z_2 + Zin + Z_4 + Z_5}$$

$$= \left(\frac{1}{1 + \frac{Z_2 + Z_4 + Z_5}{Zin}}\right) \times (A`-B`+HCP_1 + HCP_2) \quad (3)$$

C. Circuit simulation

We simulated the influence of impedance change in the equivalent circuit model by using a circuit simulation tool (p-spice, Figure 3). The simulation employed the R; the C component values were obtained from the literature and experimentation. The feasibility of the proposed method was evaluated by decreasing Z5 (to 1 ohm, 10 ohm, 100 ohm, 1 kohm, and 10 kohm). HCP variation was set with the sine wave at 1 Hz.

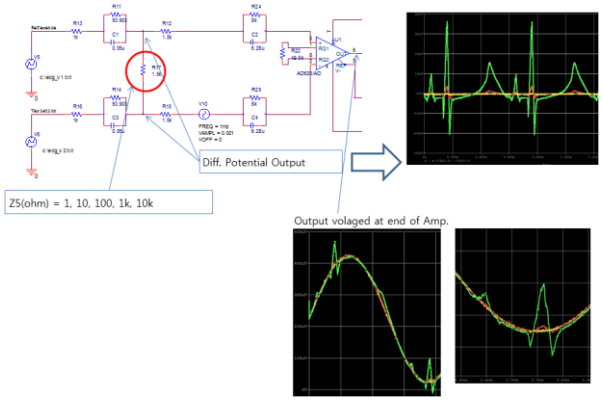

Figure 3. Circuit simulation to evaluate the influence of Z5

D. Experimental protocol: correlation study

The customized measurement device has two-channel (2CH) instrumental amplifiers, a CPU, a wireless data communication module, and a battery. The two channels are the ECG channel and the HCP channel. The sensing device and 2CH electrode are shown in Fig 4. The continuous 2CH signal was recorded by a computer through wireless communication.

To evaluate the correlation coefficients between data from ECG CH and HCP CH, the sensing device was placed on the subject's arm. Then the defined four motions (push, pull, stretch, and shake) were applied around the skin to induce motion artifacts. Combined with these simple motions were local changes in the skin and electrode interface that induce motion noise during such daily activities as walking and running.

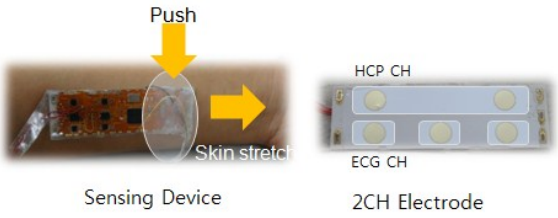

Figure 4. System implementation using 2CH electrode

In each motion category, data acquisition was performed repeatedly, 10 times. Correlational analysis was conducted with the repeated data obtained from 10 subjects.

E. Adaptive filtering

To evaluate adaptive-filtering performance, it was assumed that motion artifacts were super-positioned in the ECG from heart. For simulation purposes, the motion artifact was added to the ECG data acquired from the chest at rest, using the same device. We employed a least mean squares (LMS) adaptive filter, and used the filter coefficients of 0.01 and 4, as shown in Fig 5

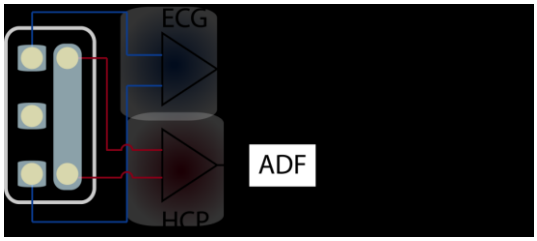

Figure 5. Motion artifact reduction using adaptive filtering

To evaluate the performance of the adaptive filtering algorithms, the signal-to-noise ratios (SNRs) before and after applying the adaptive filter were compared. In order to optimize filter coefficients, we used two metrics, the SNR and the artifact-reduction percentage (ARP).

III. RESULTS

A. *Circuit simulation results*

With the decreasing resistance value of Z5, the measurement amplitude of the ECG signal from heart the decreased, as shown in Figure 6. If the resistance was less than 1 kohm, the ECG signal was attenuated to less than 1% of the output when there was no Z5. The Z5 was near zero; the measured signal from HCP CH included only the differential potential occurring from interface changes, except for the signal from the heart (TABLE 1). Based on the simulation results, the 2CH electrode and sensing device was designed as shown in Fig 4.

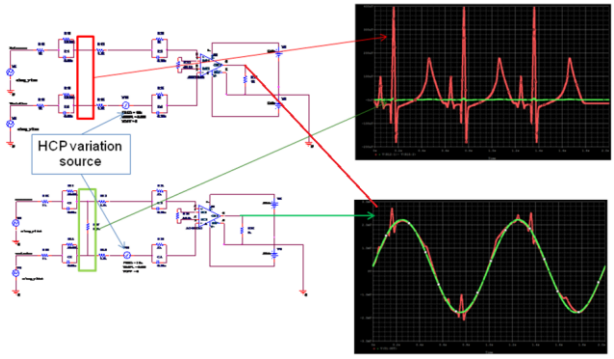

Figure 6. Bioelectric signal measurement from the proposed spice model: Red line is the measured signal from ECG CH; the green line is the signal from HCP CH.

TABLE I. DIFFERENTIAL POTENTIAL % COMPARED TO INPUT SIGNAL

Z5 (Ohm)	Differential Potential % compared to input signal
1	0.0005
10	0.005
100	0.05
1k	0.5
10k	4.8

B. *Correlation results (between MA and HCP)*

Depending on the changes applied to the skin–electrode interface, the correlation coefficient varied between 0.44 and 0.99 ($r = 0.75 \pm 0.18$; $n = 10$). The correlation coefficient was 0.99 when one side of the system was pushed and released repeatedly for 10 seconds. There was no consistent correlation between the HCP variation detected by the modified electrode and the amplitude of the ECG artifacts shown in Fig 7. The signal amplitudes and correlation coefficients changed depending on the displacement of skin around the electrode.

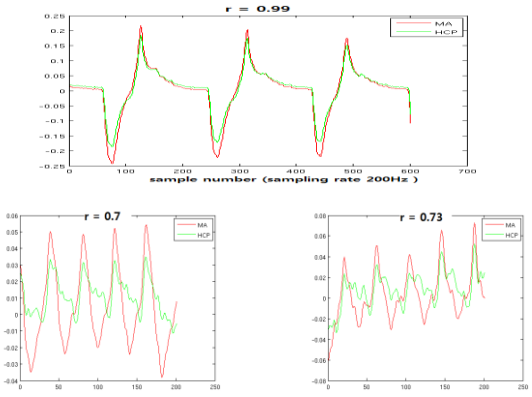

Figure 7. Experimental results: correlation coefficients between HCP CH(green line) and ECG CH(red line)

C. *Performance of adaptive filtering*

The noisy ECG was made with an artifact-free ECG by adding the motion artifacts measured on the subject's arm. After adaptive filtering using the calculated signal and reference signal from HCP CH, the average SNR was increased from 3.7 dB to 6.7 dB. If the SNR was larger than 6 dB, the accuracy of R-peak detection could be over 90%. When a reference signal having a low correlation ($r < 0.7$) with the motion artifacts was used with the adaptive filter, the reduction performance of the filter was less than 40%, as seen in Fig 8.

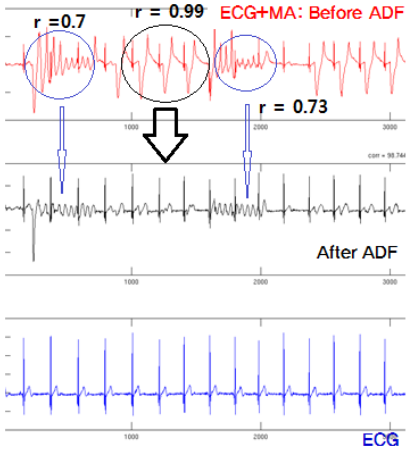

Figure 8. Performance of adaptive filter

IV. Discussion

In this study, we obtained correlation coefficients from signals measured on the arm using the proposed sensing device and evaluated the effect of artifact reduction through numerical simulation. When the correlation coefficient is high, ARP rises (Fig 9). We successfully used the ARP metric suggested by Liu [5] to evaluate the performance of our adaptive filtering method.

The major causes of motion artifacts are changes in the impedance and the half-cell potential originating from changes in the skin–electrode interface. The influence of the impedance change is very small because the impedances from Z1–Z4 are so small (less than 1%), as compared with the input impedance (10 Mohm). When the impedance of all elements fluctuates between 50% and 150%, the noise level via the desired signal is only 0.73%. The typical half-cell potential values are much larger than the desired measurement signals (HCP: 0.1–0.5 V vs. ECG: 1–2 mV). The noise from HCP variations overlap each other, rendering the desired signals without attenuation. Then, the imbalance of HCP (HCP1–HCP2) has larger amplitude than the ECG signal.

In this paper, we have proposed a modified bipolar electrode for eliminating motion artifacts when taking ECG measurements during daily activities and exercise. We found that changing the interface of the two channels was the same as having a high correlation coefficient. However, the imbalance in load distribution when the skin stretches causes a phase delay between the two signals whereby the correlation is degraded.

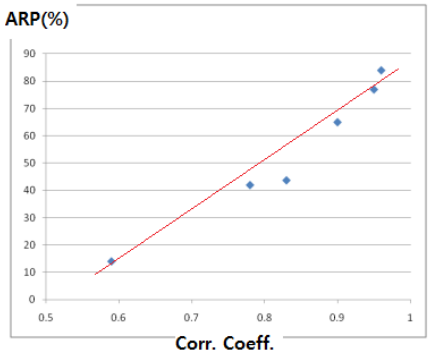

Figure 9. ARP according to correlation coefficients

The limits of the proposed electrode for 1CH ECG measurement require an additional channel to monitor motion artifacts. Because two channels are spatially separated, a high degree of correlation can be guaranteed by a uniform load distribution. However, direct measurement of motion artifacts uses the same path as that used for ECG monitoring, so a higher correlation can be expected from using additional sensors. High-quality ECG signals acquisition will improve diagnostic accuracy and can contribute to the improved performance of heart-rate monitors for both casual and experienced athletes.

References

[1] "An Unhealthy America: The Economic Burden of Chronic Disease," Http://www.chronicdiseaseimpact.com

[2] W Liu, Y Chen, C Chen, Y Lu , "A tele-healthcare framework implementation for family and community," *IT in Medicine and Education*, vol.1, pp.267-271, Dec. 2011

[3] H Lee, S Lee, K Ha, H Jang, W Chung, J Kim, Y Chang, D Yoo, "Ubiquitous healthcare service using Zigbee and mobile phone for elderly patients," *International Journal of Medical Informatics*, Vol 78, Issue 3, pp.193-198, Mar. 2009

[4] G.M. Friesen, T.C. Jannett, M.A. Jadallah, S.L. Yates, S.R. Quint, H.T. Nagle, "A comparison of the noise sensitivity of nine QRS detection algorithms," *IEEE Transactions on Biomedical Engineering*, vol.37, no.1, pp.85-98, Jan. 1990

[5] Y. Liu, "Reduction of skin stretch induced motion artifacts in electrocardiogram monitoring using adaptive filtering", Ph.D. dissertation, Dept. Mech. Eng., Univ. of Maryland, College Park, MD, 2007.

[6] P.S. Hamilton, M.G. Curley, R.M. Aimi, C. Sae-Hau, "Comparison of methods for adaptive removal of motion artifact," *Computers in Cardiology*, pp.383-386, 2000

[7] M.A.D. Raya, L.G. Sison , "Adaptive noise cancelling of motion artifact in stress ECG signals using accelerometer," in *2002 Proc. EMBS/BMES Conf.*, vol.2, pp. 1756- 1757

[8] X Pengjun; T Xiaoming; W Shanyuan; , "Measurement of wearable electrode and skin mechanical interaction using displacement and pressure sensors," in *2011 Proc. BMEI Conf.*, vol.2, pp.1131-1134

[9] Y Kim, ,K Lim, S Hong, A Ryu, B Ko, S Bae, K Shin, E Shim, "Numerical simulation of motion-induced dynamic noise in a ubiquitous ECG application," in *2011 Proc., EMBC*, pp.997-1000

[10] A. B. Simakov and J. G. Webster, "Motion Artifact from Electrodes and Cables," *IRANIAN J. Elect. Comp. Eng.*, Vol. 9, No. 2, pp. 139–143, 2010